

Comparison of the phonon spectra of ^{70}Ge and natural Ge crystals: Effects of isotopic disorder

H. D. Fuchs, C. H. Grein, C. Thomsen, and M. Cardona
*Max-Planck-Institut für Festkörperforschung, Heisenbergstrasse 1,
D-7000 Stuttgart 80, Federal Republic of Germany*

W. L. Hansen
Lawrence Berkeley Laboratory, Berkeley, California 94720

E. E. Haller and K. Itoh
*University of California, Berkeley, California 94720
and Lawrence Berkeley Laboratory, Berkeley, California 94720*
(Received 8 October 1990)

The difference in phonon energies and broadenings between an isotopically enriched crystal of ^{70}Ge (95.9%) and a germanium crystal of natural isotopic composition was measured with high accuracy in first- and second-order Raman spectra (with laser excitation energies of $E_L = 2.41$ eV and $E_L = 2.183$ eV, respectively) and compared to coherent-potential-approximation and lowest-order perturbation-theory calculations. The energy of the first-order $O(\Gamma)$ phonon shifts up by 4.9 ± 0.1 cm^{-1} in the isotopically pure crystal, in good agreement with the calculated value of 4.3 ± 0.4 cm^{-1} . No broadening due to isotopic disorder was observed for optical phonons at the Γ point [full width at half maximum (FWHM) of 0.99 ± 0.03 cm^{-1} at 80 K for both crystals]. However, additional broadening at the W and L point was found in the second-order Raman spectra (FWHM broadening of 6.5 ± 0.5 cm^{-1} at the L point). This broadening and the shifts of the acoustic- and optical-phonon peaks in the second-order spectra agree well with calculations of the phonon overtone density of states.

I. INTRODUCTION

The effect of isotopic disorder on properties of crystalline materials has attracted considerable interest in the past from both theoretical and experimental points of view.¹ Properties such as the phonon spectra (phonon energies and broadenings), the unit-cell volume, the atomic hopping mobility, and the anharmonicity depend on the isotope distribution in the material. This means that all material characteristics that depend on these properties are also isotope dependent. Examples for such isotope-dependent characteristics are thermal conductivity, thermal expansion, melting temperatures, T_c of superconductivity, nuclear magnetic resonance (NMR), and Raman spectra.

Tamura² theoretically investigated the isotope scattering of near-zone-boundary acoustic phonons in germanium in the THz region. He calculated the frequency shifts due to isotopic disorder using a Born-von Kármán model of lattice dynamics and the first Born approximation. Because no experimental data were available, these theoretical results could not be compared with any measurements.

A scaling theory was developed by Kazakovtsek and Levinson³⁻⁵ to describe nonequilibrium phonon propagation in a crystal. In this theory two types of scattering processes are considered: elastic scattering (due to isotopic disorder and other defects) and spontaneous anharmonic decay. However, using Monte Carlo calculations, Maris⁶ has recently shown that this theory may be invalid in the case of crystals in which the scattering of phonons arises only from different naturally occurring isotopes.

Other theoretical work has dealt with the frequently made assumption of a perfectly random distribution of different stable isotopes among lattice sites.⁷ Instead of perfect randomness, ordering on the basis of spontaneous pattern formation in nonlinear systems⁸ has been proposed. To our knowledge there is no evidence of clustering in germanium, thus a random distribution of the various germanium isotopes is assumed in this work.

In addition to theoretical research, experimental results of isotopic effects have also been reported in the past. Experimentally found asymmetric absorption line shapes in organic crystals^{9,10} are in agreement with a theory¹¹ which includes both structural disorder (isotopes) and weak electron-phonon coupling effects.

TABLE I. Isotopic composition of isotopically enriched ^{70}Ge and natural Ge used in this experiment.^a

Isotope	Mass (a.u.) ^b	Atomic percent	
		Isotopically enriched ^{70}Ge	Natural Ge
70	69.9243	95.9	22.1
72	71.9217	3.8	28.0
73	72.9234		7.86
74	73.9219		34.7
76	75.9214		7.1

^aReference 22.

^bReference 34.

Optical-absorption and luminescence measurements on ^{13}C and ^{12}C diamonds^{12,13} show that the indirect energy gap is 13.6 ± 0.2 meV higher for ^{13}C than for ^{12}C diamonds. The differences of the energy gap arise mainly from the isotopic dependence of the electron-phonon coupling and a smaller, but significant, contribution from the dependence of the atomic spacing on the isotopic composition.

In germanium, where the fractional differences in the isotopic masses are considerably smaller than in diamond, the variation of lattice parameters between crystals of natural isotopic composition and a crystal of ^{74}Ge was measured recently.¹⁴

The earliest published measurements on isotopic effects in germanium go back to 1958, when Geballe and Hull compared the thermal conductivity of ^{74}Ge with natural germanium,¹⁵ confirming the theory of Klemens¹⁶ and Pommeranchuk.¹⁷⁻¹⁹ Much later, Ye *et al.*²⁰ used time-resolved picosecond Raman spectroscopy²¹ to measure the relaxation rate of a nonequilibrium population of zone-center TO phonons in germanium. Comparing their results with experimental data for the temperature dependence of phonon linewidths of Raman spectra,²² they attributed the difference between the relaxation time and the phonon lifetime (inverse of linewidths) to isotopic disorder in the germanium crystal.

In this paper we investigate more directly the effect of isotopic disorder on vibrational Raman spectra in germanium by comparing spectra of a crystal of natural isotopic composition with those of isotopically enriched ^{70}Ge (95.9%), taken under identical conditions with laser excitation energies of $E_L = 2.41$ and 2.183 eV. The isotopic composition of our isotopically enriched ^{70}Ge crystal is given in Table I, obtained by means of mass spectroscopy.²³ Since the portion of the isotope ^{70}Ge in the enriched sample is 95.9%, we will refer to this crystal as the " ^{70}Ge sample" in the following sections of this paper.

The phonon energies as well as their broadening are investigated theoretically (Sec. II), using the coherent-potential approximation and low-order perturbation-theory calculations, and experimentally (Sec. III). The calculated shifts of the phonon energies, arising mainly from the differences in the average isotopic mass and a smaller contribution from self-energy corrections due to isotopic disorder, agree well with the measured values (Sec. IV). There is no broadening due to isotopic disorder

for phonons at the Γ point, as opposed to the L and W point where isotopic broadening could be measured.

II. THEORY

In this section, two methods which we have employed to evaluate phonon energy shifts and broadenings due to isotopic disorder are described. The first is the coherent potential approximation, and the second lowest-order perturbation theory.

In tetrahedrally coordinated semiconductors the second-order vibrational Raman spectrum for parallel incident and scattered photon polarizations follows closely the phonon overtone density of states. Therefore our first approach is to evaluate the effects of isotopic disorder on the overtone density of states by means of the coherent-potential approximation (CPA),^{24,25} and compare the results of this calculation directly with the second-order Raman spectra. By using the CPA, the usual approximations inherent in this method are made, mainly that only the effects of differences in isotopic masses are taken into account (not force-constant changes), and that the isotopes are randomly distributed on the lattice (not clustered). We find that self-energy corrections due to isotopic disorder for certain phonons may be quite large, thus a multiple scattering formalism such as the CPA is expected to provide a more accurate estimation of such corrections than lowest-order perturbation theory.

In the usual formulation of the CPA only scattering by a single type of impurity is considered, but it is easily generalized to treat scattering by any number of impurities. However, the CPA equations are more difficult to solve the larger the number of impurities, thus we have simplified the problem by considering only scattering by the three highest concentration isotopes ^{70}Ge , ^{72}Ge , and ^{74}Ge . The effects of the other isotopes are small due to their low concentration.

We treat scattering in the CPA with respect to the virtual crystal (VC), defined to be a perfect diamond-structure crystal with each site occupied by an atom of atomic mass equal to the concentration-weighted average isotopic mass. In the VC, the phonon frequencies are given by ω_{qj} , where q is the wave vector and j the branch index. Scattering is treated by considering an effective medium characterized by the dimensionless "self-energy"

$\xi(\omega)$ with respect to the VC, where we employ the notation of Ref. 24. In this medium, the CPA condition for zero average scattering at a single site takes the form

$$\sum_{i=1}^3 \frac{x_i \{M_{\text{VCA}} \omega^2 [1 - \xi(\omega)] - M_i \omega^2\}}{1 - \{M_{\text{VCA}} \omega^2 [1 - \xi(\omega)] - M_i \omega^2\} G_M(0,0;\omega^2)} = 0, \quad (2.1)$$

where the concentration of the three isotopes x_1 , x_2 , and x_3 sum to 1; M_1 , M_2 , and M_3 are their respective masses; and the VC mass is $M_{\text{VCA}} = x_1 M_1 + x_2 M_2 + x_3 M_3$. G_M is the site Green's function in the effective medium [solving Dyson's equation to lowest order in $\xi(\omega)$]:

$$G_M(0,0;\omega^2) = \frac{1}{NM_{\text{VCA}}} \sum_{qj} \frac{1}{\omega^2 [1 - \xi(\omega)] - \omega_{qj}^2}, \quad (2.2)$$

where N is six times the number of unit cells in the VC. Equations (2.1) and (2.2) must be solved self-consistently for the complex self-energy $\xi(\omega)$. The one-phonon density of states is then given by

$$\rho(\omega) = -\frac{2}{N\pi\omega} \sum_{qj} \omega_{qj}^2 \text{Im} \{ \omega^2 [1 - \xi(\omega)] - \omega_{qj}^2 \}^{-1}, \quad (2.3)$$

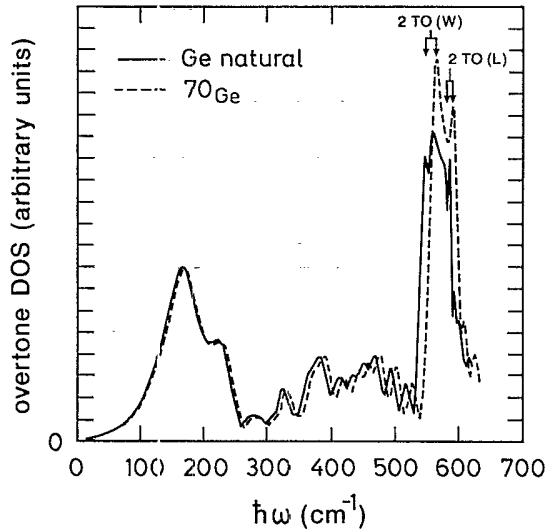


FIG. 1. Calculated overtone phonon density of states of ^{70}Ge compared with natural Ge. The natural Ge curve takes into account multiple-scattering corrections within the coherent-potential approximation. The density of states has been smoothed to eliminate some numerical noise, however the plot gives accurate shifts and broadenings.

and the overtone density of states is obtained by doubling the frequency.

The CPA equations were solved numerically as follows. The phonon frequencies in the VC were obtained using Weber's bond-charge model parametrization²⁶ with the mass M_{VCA} on every site. The summation in (2.2) was performed over 505 q points in an irreducible $\frac{1}{48}$ wedge of the Brillouin zone, and all six phonon branches. The evaluation of (2.2) was facilitated by shifting ω^2 well above the real axis, in which case the summation converges rapidly, and then analytically continuing back to real frequencies.²⁷ Self-consistency was achieved by evaluating (2.2) for an initial guess for the self-energy, using this to solve (2.1) for a new self-energy and repeating until the values of the self-energy have converged. Equation (2.1) is then cubic in the self-energy; care must be taken to iterate the correct root.

In Fig. 1, a comparison is made between the bond-charge model overtone density of states of ^{70}Ge and natural Ge, the latter obtained with CPA corrections. It shows that the dominant effects of isotopic disorder take place on the high-frequency optical phonons. With respect to the wide peak bounded by the 2TO(W) and 2TO(L) phonons of ^{70}Ge , this peak in natural Ge is broadened [full width at half maximum (FWHM)] by 6.0 cm^{-1} . These results are compared with experimental second-order Raman spectra in Sec. IV.

Figure 2 displays the calculated CPA self-energy of natural Ge with respect to the virtual crystal. The effects

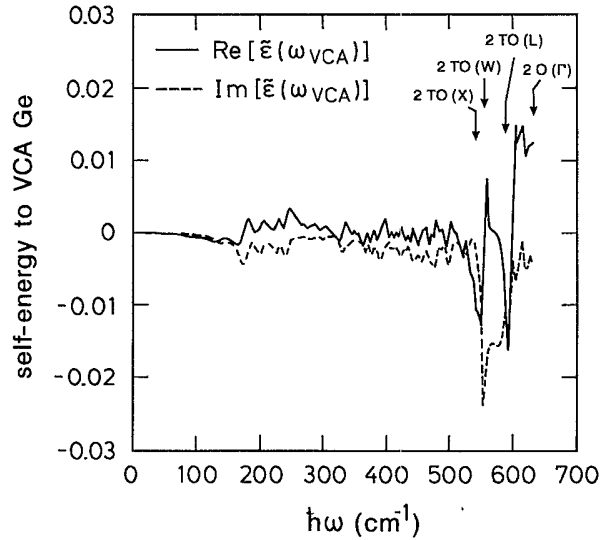


FIG. 2. Complex self-energy ξ of natural Ge with respect to virtual-crystal Ge, calculated in the coherent-potential approximation to take into account the effects of isotopic disorder. The shifted frequency is approximately given by $\omega_{\text{CPA}} \approx \omega_{\text{VCA}} / \sqrt{1 - \text{Re}\xi(\omega_{\text{VCA}})}$, and the FWHM broadening by $-\omega_{\text{CPA}} \text{Im}\xi(\omega_{\text{CPA}})$, where ω_{VCA} is the phonon frequency in the virtual crystal.

of isotopic disorder result in the frequency being shifted to $\omega_{\text{CPA}} = \omega_{\text{VCA}} / \sqrt{1 - \text{Re}\tilde{\epsilon}(\omega_{\text{CPA}})}$ [which may be approximated by $\omega_{\text{CPA}} = \omega_{\text{VCA}} / \sqrt{1 - \text{Re}\tilde{\epsilon}(\omega_{\text{VCA}})}$] and a FWHM broadening of $-\omega_{\text{CPA}} \text{Im}\tilde{\epsilon}(\omega_{\text{CPA}})$.

The first-order Raman spectrum contains the contributions of $O(\Gamma)$ phonons at frequency $\hbar\omega_{\text{Optical}} \sim 310 \text{ cm}^{-1}$. The calculated frequency shift of this line in natural Ge with respect to its position in ^{70}Ge has two contributions, the first due to isotopic disorder on VC Ge and the second due to the mass difference between the VC Ge and ^{70}Ge , the former being obtained from the CPA. We calculate a downward shift of

$$\begin{aligned} & \Delta\hbar\omega_{\text{CPA}} + \Delta\hbar\omega_{\text{mass}} \\ &= \hbar\omega_{\text{Optical}} \left\{ \left[1 / \sqrt{1 - \text{Re}\tilde{\epsilon}(\omega_{\text{Optical}})} - 1 \right] \right. \\ & \quad \left. - \left(\sqrt{M_{\text{VCA}} / M_{^{70}\text{Ge}}} - 1 \right) \right\} \\ &= 1.5 \text{ cm}^{-1} - 5.8 \text{ cm}^{-1} = -4.3 \text{ cm}^{-1}, \end{aligned}$$

but no reliable values can be reached for the broadening due to numerical noise. As the density of states approaches zero at Γ , the imaginary part of the self-energy also approaches zero; thus the broadening is expected to be small.

To obtain a more accurate estimate of the broadening of the $O(\Gamma)$ line, a perturbative method is employed. Since the self-energy is small near Γ , lowest-order perturbation theory should give an accurate estimate. The basis of the method is the self-consistent Born approximation

$$\begin{aligned} \Gamma_{\text{imp}}(\omega) &= 3\pi \sum_{\mathbf{q}j} \langle \Gamma, \text{optical} | H_{\text{scatt}} | \mathbf{q}j \rangle|^2 \\ & \quad \times \delta[\hbar\omega - \hbar\omega_{\mathbf{q}j} + i\Gamma_{\text{ph}} + i\Gamma_{\text{imp}}(\omega)] \end{aligned} \quad (2.4)$$

for the half width at half maximum broadening Γ_{imp} due to isotopic disorder of the threefold-degenerate $O(\Gamma)$ phonons at frequency ω , where Γ_{ph} represents the broadening due to spontaneous anharmonic decay of the optical phonon. The contribution of Γ_{ph} to the broadening was neglected in the CPA calculations above. Equation (1.4) must be solved self-consistently for Γ_{imp} . Related calculations without the self-consistency requirement are performed in Refs. 2 and 20; these other methods, however, will give no broadening to a phonon at Γ (or only broadening due to Γ_{ph}) due to the vanishing of the phonon density of states. Equation (2.4) may be approximated by

$$\begin{aligned} & \Gamma_{\text{imp}}(\omega_{\text{Optical}}) \\ & \approx 3\pi \langle \Gamma, \text{optical} | H_{\text{scatt}} | \Gamma, \text{optical} \rangle|^2 \\ & \quad \times \text{Re}\rho[-i\Gamma_{\text{ph}} - i\Gamma_{\text{imp}}(\omega_{\text{Optical}})], \end{aligned} \quad (2.5a)$$

where²

$$\begin{aligned} & |\langle \Gamma, \text{optical} | H_{\text{scatt}} | \Gamma, \text{optical} \rangle|^2 \\ &= \frac{1}{6} \sum_i x_i (\hbar\omega_{\text{Optical}})^2 \left[\frac{M_i - M_{\text{VCA}}}{2M_{\text{VCA}}} \right]. \end{aligned} \quad (2.5b)$$

Here the sum runs over the various isotopes. The form of H_{scatt} follows from the assumption that the local phonon-energy change due to the replacement of a site mass M_{VCA} with a nearly equal mass M_i is

$$\begin{aligned} \Delta\hbar\omega &= \hbar\sqrt{k/M_i} - \hbar\sqrt{k/M_{\text{VCA}}} \\ & \approx \hbar\omega_{\text{VCA}} [(M_i - M_{\text{VCA}}) / 2M_{\text{VCA}}], \end{aligned}$$

where k is an effective spring constant. The optical-phonon density of states ρ near Γ was obtained from recent calculations of the phonon-dispersion relationships;²⁸ we employed $\rho(\hbar\omega) = 559(\hbar\omega_{\text{Optical}} - \hbar\omega)^{1/2}$ states per unit cell per eV, where the phonon energies are in eV.

We have evaluated (2.5) using $\Gamma_{\text{ph}} = 0.495 \text{ cm}^{-1}$ (as obtained in Sec. III), and summing (2.5b) over the five highest concentration isotopes. This calculation gives $\Gamma_{\text{imp}} = 0.0085 \text{ cm}^{-1}$, much less than Γ_{ph} . Thus the $O(\Gamma)$ linewidth is not expected to be significantly broader in natural Ge than in ^{70}Ge .

III. EXPERIMENT

A. Experimental details

The germanium sample of natural isotopic compositions was cut in the (111) orientation from a high-purity nearly intrinsic single crystal. The starting material for the isotopically enriched ^{70}Ge crystal, used in this experiment, was coarse polycrystalline ^{70}Ge powder with a 25% GeO content. The Ge was enriched to 96% ^{70}Ge , with the remaining 4% being ^{72}Ge , and the powder was cast into a solid polycrystalline Ge slug, 6 mm in diameter. Using the vertical Bridgman technique with a programmed temperature ramp, a single crystal was grown in a carbon smoke coated split graphite crucible with a long, thin seeding section. The growth ambient was H_2 .

The chemomechanically polished surface of both the ^{70}Ge and the isotopically natural crystal was cleaned with diethyl-ether and acetone prior to measurements being taken. Raman spectra were recorded in a backscattering geometry with parallel incident and scattered polarization at liquid-nitrogen temperature using the discrete lines of Ar^+ - and Kr^+ -ion lasers at wavelengths of 514.5 and 586.2 nm, respectively. A series of measurements of phonon spectra was performed with varying slit widths

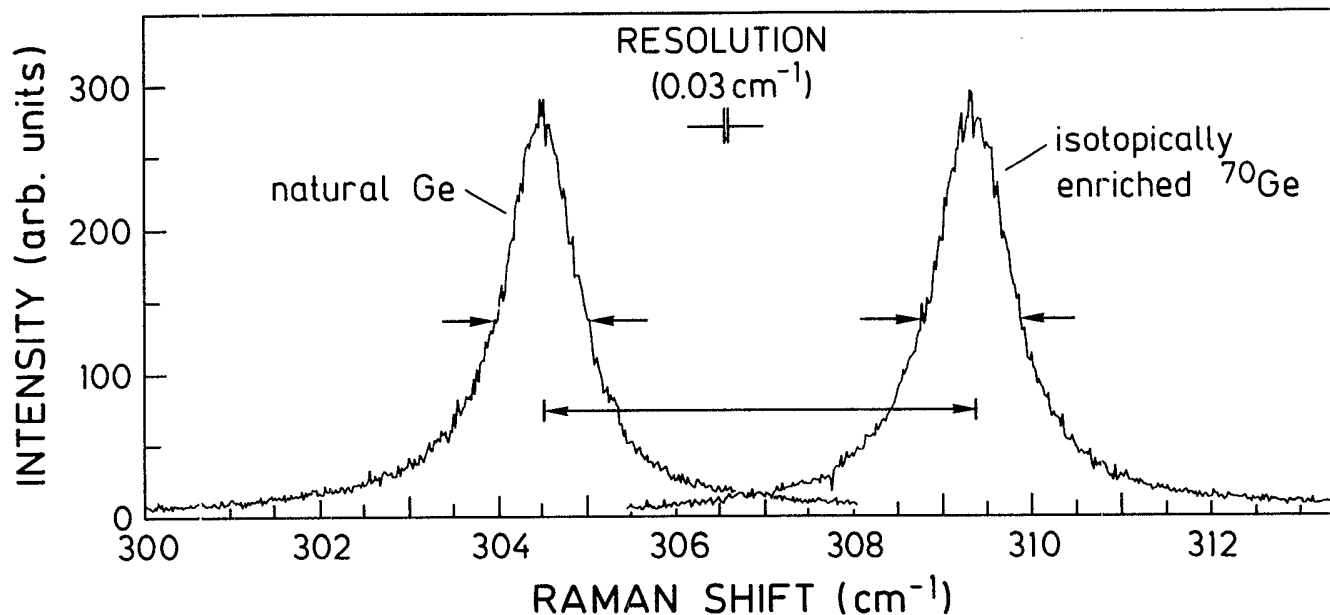


FIG. 3. First-order Raman spectra of isotopically enriched ^{70}Ge (95.9%) and natural germanium. No difference in the broadening can be observed within the experimental uncertainty. Shift and broadening of the spectra are discussed in the text. Data were taken at 80 K in tenth order of a 2.12-m Sopra double monochromator with an excitation energy of $E_L = 2.41$ eV (Ar⁺ laser with étalon).

on a 0.75-m SPEX double monochromator using conventional photon-counting techniques (PM). In order to obtain high-accuracy data with less instrumental broadening, the first-order spectra were recorded again, this time using a 2.12-m Sopra double monochromator (single-pass configuration). An étalon was placed in the cavity of the Ar⁺-ion laser, and the spectra were recorded in the tenth diffraction order of the grating. The resulting laser

linewidth of 0.134 cm^{-1} (FWHM), measured with the same slit apertures as the Raman experiment, indicates an uncertainty of about 0.03 cm^{-1} for the broadening.

The second-order phonon spectra were taken with a DILOR-XY triple monochromator in subtractive mode and a multichannel detection system (charge-coupled-device camera, cooled to 160 K) because of the high response of this instrument. To enhance the instrumental

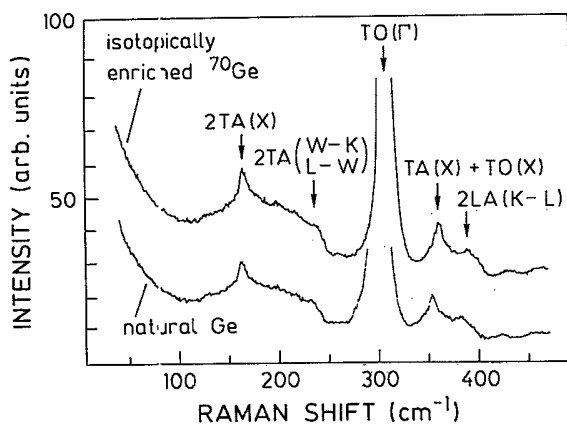


FIG. 4. Second-order acoustic overtone and combination Raman spectrum of isotopically enriched ^{70}Ge (upper curve) compared to natural germanium (lower curve). The observed peak positions are listed in Table II. Data were taken at 80 K with a laser excitation energy of $E_L = 2.183$ eV.

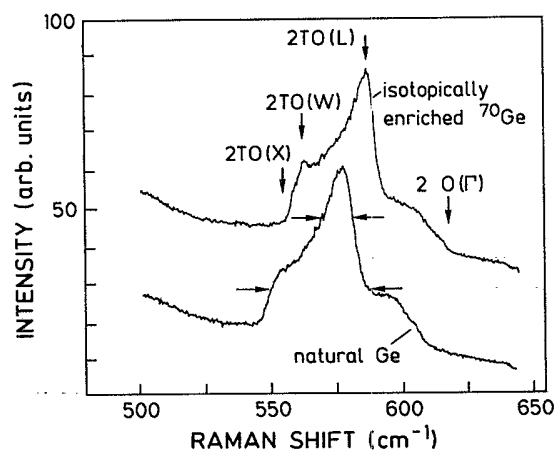


FIG. 5. Second-order optical Raman spectrum of isotopically enriched ^{70}Ge (upper curve) and natural germanium (lower curve). The observed peak positions are listed in Table II and the arrows indicate the linewidths discussed in the text. Data were taken at 80 K with a laser excitation energy of $E_L = 2.183$ eV.

TABLE II. Observed peaks in the second-order Raman spectra of isotopically enriched ^{70}Ge and natural Ge (from Figs. 4 and 5), with frequency shifts compared to coherent-potential-approximation (CPA) calculations.

Identification	Phonon energies (cm^{-1})			Relative shift of phonon energy (%)	
	in ^{70}Ge Expt.	in natural Ge Expt.	CPA	Expt.	CPA
2TA(X)	165.1	162.5	161.8	1.6	2.0
2TA(W-K, L-W)	235.9	231.2	231.5	2.0	2.0
O(Γ)	309.4	304.5	304.8	1.6	1.4
TO(X)+TA(X)	361.1	354.6	354.0	1.7	1.9
2LA(K-L)	389.8	382.3	382.1	1.9	2.0
2TO(X)	554.8	546.0	542.5	1.6	2.2
2TO(W)	562.8	553.6	553.9	1.7	1.6
2TO(L)	586.7	577.5	575.2	1.6	2.0
2O(Γ)	618.8	609.0	609.6	1.6	1.4

^aReference 31.

resolution but maintain the high sensitivity, this system was run again in triple additive mode.

B. Experimental results

The spectra of the first-order optical phonons (Fig. 3) display a phonon-energy shift by 4.9 cm^{-1} from 304.5 cm^{-1} for natural Ge to 309.4 cm^{-1} for ^{70}Ge . The broadening of the peaks is identical for ^{70}Ge and natural Ge (FWHM of 1.008 cm^{-1}), within the uncertainty of the measurement (0.03 cm^{-1}).

Even though the spectrometer allows extremely accurate measurements, the finite resolution of the system has to be taken into account. This instrumental function of a nonideal spectrometer can be approximated by a Gaussian.²⁹ The convolution of a Gaussian with a Lorentzian curve is a Voigt profile,³⁰ which is indistinguishable from a Lorentzian for signal-to-noise ratios smaller than 100.³² We therefore fitted the experimental peaks with a Lorentzian function, and the FWHM we obtained was assumed to be equal to the FWHM one would find by fitting the experimental peaks with a Voigt profile.²² After the fitting we corrected for the finite resolution of the spectrometer by using Posener's table³⁰ and obtained a linewidth of $0.99 \pm 0.03 \text{ cm}^{-1}$ for both the natural Ge and ^{70}Ge at 80 K. For the width of the response function of the spectrometer, the above-mentioned laser linewidth of 0.134 cm^{-1} (FWHM) was taken. Additional measurements with a 0.75-m SPEX double monochromator for slit widths varying from 300 to $35 \mu\text{m}$ yield an average deconvoluted phonon linewidth of $0.97 \pm 0.1 \text{ cm}^{-1}$ at 80 K for both ^{70}Ge and natural germanium.

Energies and broadenings for phonons away from the zone center ($q \neq 0$) were obtained from acoustic and optical two-phonon spectra (Figs. 4 and 5). As opposed to the phonons at the Γ point in the first-order spectra, the 2TO(W)- and 2TO(L)-phonon peaks are broader in natural Ge than in ^{70}Ge .

The experimental line shape of the 2TO(L) phonons (Fig. 5) of natural Ge can be reproduced by convoluting this line in ^{70}Ge with a Gaussian of $6.5 \pm 0.5 \text{ cm}^{-1}$ (FWHM). The phonons of the W point are not clearly resolved, but the structure consisting of both L- and W-point phonons shows for the natural germanium an additional broadening of about 10 cm^{-1} with respect to ^{70}Ge . These spectra display an intermediate resonant state for 2TO(L) for laser excitation energy near $E_L = 2.183 \text{ eV}$. The acoustic two-phonon spectra (Fig. 4) are too weak for a precise analysis of the linewidths.

As with the first-order spectra, the overtone and combination spectra (Figs. 4 and 5) display shifts of the ^{70}Ge phonons to higher energies with respect to natural Ge. The observed two-phonon peaks, of both the isotopically enriched ^{70}Ge and natural Ge, and their relative shifts are listed in Table II.

IV. DISCUSSION AND SUMMARY

A direct comparison between Raman spectra and overtone density of states cannot be done with great precision because the Raman scattering efficiency is the combination and overtone phonon density of states weighted by electron-phonon and electron-photon matrix elements and energy denominators.³³ For tetrahedrally coordinated semiconductors those matrix elements in the second-order spectra involving phonon overtones dominate the scattering efficiency and, away from resonance, vary weakly with Raman frequency shift; thus second-order spectra are a good measure of the overtone density of states. It must be kept in mind, however, that resonant intermediate states will in general distort the shape of Raman spectra away from that of the density of states.

Considering the first-order Raman spectra, the O(Γ) peak shifts downward by $4.9 \pm 0.1 \text{ cm}^{-1}$ going from ^{70}Ge to natural Ge, in good agreement with the calculated

value of $4.3 \pm 0.4 \text{ cm}^{-1}$. The observed broadening of this peak is the same in natural Ge and ^{70}Ge ($0.99 \pm 0.03 \text{ cm}^{-1}$ at 80 K), as is predicted by second-order perturbation theory.

Turning to the second-order spectra, Table II summarizes the observed shifts of peak positions. Agreement with the calculated shifts, also in Table II, is good. The experimental signal-to-noise ratio is too weak to obtain accurate broadenings in the acoustic-phonon region of the spectrum, and the calculations indicate that the broadenings are negligible here. A comparison between theoretical and experimental broadenings for the optical-phonon peaks is less accurate since the Raman spectra are dominated by intermediate-state resonances involving $2\text{TO}(L)$ phonons. The observed FWHM broadening of the wide $2\text{TO}(W)$ and $2\text{TO}(L)$ structure in natural Ge is about 10.0 cm^{-1} greater than in ^{70}Ge and about 4.2 cm^{-1} at 80% full maximum. The calculated overtone density of states for this structure in natural Ge has a FWHM broadening of 6.0 cm^{-1} greater than in ^{70}Ge . Convoluting the experimental $2\text{TO}(L)$ peak in ^{70}Ge with a Gaussian to give the natural Ge peak reveals an additional FWHM broadening of $6.5 \pm 0.5 \text{ cm}^{-1}$ due to disorder; whereas Fig. 2 indicates that the calculated disorder-induced FWHM broadening of this peak is about $8.3 \pm 0.9 \text{ cm}^{-1}$.

Thus, upon comparing natural Ge and ^{70}Ge , we find general agreement between the calculated and measured

linewidths and line shifts. We conclude that the observed effects are accounted for by the effects of isotopic disorder in natural Ge.

After completing this paper we became aware of recent measurements of the edge photoluminescence, absorption, and first-order Raman scattering in ^{70}Ge compared to natural Ge.³⁵ This work complements our measurements of the first- and second-order Raman spectra of ^{70}Ge .

Note added in proof. Recent investigation revealed an asymmetry of the first-order Raman spectra for ^{70}Ge as well as for natural Ge. The linewidth of pure ^{70}Ge was found to be larger than that of natural Ge by about 3.7%, which can be explained with the mass dependence of the anharmonic decay time of optical phonons. This will be discussed in detail in a subsequent publication.

ACKNOWLEDGMENTS

We gratefully acknowledge Professor V. Ozhigin of the Kurchatov Institute of Moscow for providing the isotopically enriched ^{70}Ge used in this experiment. We are also thankful to P. Knoll, D. M. Mowbray, and B. Friedl for many useful discussions and to M. Siemers, P. Wurster, and H. Hirt for technical assistance. C. G. acknowledges partial support of the Natural Sciences and Engineering Research Council of Canada.

- ¹A recent review is found in A. A. Berezin and A. M. Ibrahim, *Mater. Chem. Phys.* **19**, 407 (1988).
- ²S. Tamura, *Phys. Rev. B* **27**, 858 (1983).
- ³D. V. Kazakovtsek and Y. B. Levinson, *Pis'ma Zh. Eksp. Teor. Fiz.* **27**, 194 (1978) [*JETP Lett.* **27**, 181 (1978)]; *Phys. Status Solidi B* **96**, 117 (1979).
- ⁴Y. B. Levinson, in *Nonequilibrium Phonons in Nonmetallic Crystals*, edited by W. Eisenmenger and A. A. Kaplyanski (North-Holland, Amsterdam, 1986).
- ⁵T. E. Wilson, F. M. Lurie, and W. E. Born, *Phys. Rev. B* **30**, 6103 (1984).
- ⁶H. J. Maris, *Phys. Rev. B* **41**, 9736 (1990).
- ⁷A. A. Berezin, *Phys. Lett. A* **138**, 447 (1989).
- ⁸H. Haken, *Synergetics* (Springer-Verlag, Berlin, 1990).
- ⁹D. M. Burland, *J. Chem. Phys.* **59**, 4283 (1973).
- ¹⁰D. M. Burland and R. M. MacFarlane, *J. Lumin.* **12**, 213 (1976).
- ¹¹J. Klafter and J. Fortner, *J. Chem. Phys.* **68**, 1513 (1978).
- ¹²A. T. Collins, S. C. Lawson, G. Davies, and H. Kanda, *Phys. Rev. Lett.* **65**, 891 (1990).
- ¹³A. T. Collins, G. Davies, H. Kanda, and G. S. Wood, *J. Phys. C* **21**, 1363 (1988).
- ¹⁴R. C. Buschert, A. E. Merlin, S. Pace, S. Rodriguez, and M. H. Grimsditch, *Phys. Rev. B* **38**, 5219 (1988).
- ¹⁵T. H. Geballe and G. W. Hull, *Phys. Rev.* **110**, 773 (1958).
- ¹⁶P. G. Klemens, *Proc. Phys. Soc. London Sect. A* **68**, 1113 (1955).
- ¹⁷I. Pomeranchuk, *J. Phys. (Moscow)* **5**, 237 (1942).
- ¹⁸P. Carruthers, *Rev. Mod. Phys.* **33**, 92 (1961).
- ¹⁹J. Callaway, *Phys. Rev.* **113**, 1047 (1959).
- ²⁰L. Ye, C. B. Roxlo, and A. Z. Genack, *Bull. Am. Phys. Soc.* **32**, 934 (1987); A. Z. Genack, L. Ye, and C. B. Roxlo, *SPIE J.* **942**, 130 (1988).
- ²¹D. V. Linde, J. Kuhl, and H. Klingenberg, *Phys. Rev. Lett.* **44**, 1505 (1980).
- ²²J. Menéndez and M. Cardona, *Phys. Rev. B* **29**, 2051 (1984).
- ²³Measurements of the isotopic composition of both natural and isotopically enriched Ge were performed at Lawrence Berkeley Laboratory.
- ²⁴D. W. Taylor, *Phys. Rev.* **156**, 1017 (1967).
- ²⁵P. Soven, *Phys. Rev.* **156**, 809 (1967).
- ²⁶W. Weber, *Phys. Rev. B* **15**, 4789 (1977); O. H. Nielsen and W. Weber, *Comput. Phys. Commun.* **18**, 101 (1979).
- ²⁷K. C. Hass, B. Velicky, and H. Ehrenreich, *Phys. Rev. B* **29**, 3697 (1984).
- ²⁸P. Molinas and M. Cardona (private communication).
- ²⁹H. J. Kostowski and A. M. Bass, *J. Opt. Soc. Am.* **46**, 1060 (1956).
- ³⁰D. W. Posener, *Aust. J. Phys.* **12**, 184 (1959).
- ³¹S. G. Sumargo, Ph.D. thesis, Universität Stuttgart, 1975.
- ³²W. J. Borer, S. S. Mitra, and K. V. Namjoshi, *Solid State Commun.* **9**, 1377 (1971).

³³For a general reference, see *Light Scattering in Solids*, edited by M. Cardona (Springer-Verlag, Berlin, 1975).

³⁴*CRC Handbook of Chemistry and Physics*, 57th ed., edited by R. C. Weast (CRC, Cleveland, 1976).

³⁵V. F. Agekyan, V. M. Asnin, A. M. Kryukov, I. I. Markov, N. A. Rud', V. I. Stepanov, and A. B. Churilov, *Fiz. Tverd. Tela (Leningrad)* **31**, 101 (1989) [*Sov. Phys.—Solid State* **31**, 2082 (1989)].